Journal of Statistical Physics, Vol. 28, No. 4, 1982

Hierarchy of Chaotic Bands

Bai-lin Hao[1,2] **and Shu-yu Zhang**[1,3]

Received November 5, 1981

Results of a detailed numerical study on the structure of chaotic bands in a forced limit cycle oscillator (the Brusselator) are presented. Embedded in the chaotic bands of primary bifurcation sequence there are many secondary sequences with both direct and inverse segments. Within secondary chaotic bands tertiary sequences of similar structure exist. This has been shown by using subharmonic stroboscopic sampling combined with power spectra analysis.

KEY WORDS: Period-doubling bifurcation; chaos; strange attractor.

1. INTRODUCTION

The occurrence of chaotic behavior in simple dynamical systems has been raising more and more interest. It is hoped to give more insight into the difficult and long-standing problem of the onset of turbulence as well as to diminish the gap between deterministic and stochastic description in physics.

For the time being most of our knowledge of chaotic behavior comes from studies on discrete nonlinear mappings. In particular, direct period-doubling bifurcation sequence, leading to inverse sequence of chaotic bands, has been observed in many one- and two-dimensional iterated maps (for a recent review see Ref. 1 and references therein). Many properties related to these mappings, such as convergence rate of the bifurcation sequences and some characteristics of the power spectra, have been shown to be universal,[1–4] i.e., independent of the detailed structure of the mapping themselves. Moreover, there have been indications that such universal properties persist for higher-dimensional systems[5] and systems described by differential equations as well.

[1] Service de Physique Théorique, CEA—Saclay, 91191 Gif-sur-Yvette Cedex, France.
[2] Permanent address: The Institute of Theoretical Physics, Academia Sinica, P.O. Box 2735, Beijing, China.
[3] The Institue of Physics, Academia Sinica, P.O. Box 603, Beijing, China.

0022-4715/82/0800-0769$03.00/0

In spite of the importance of differential equations in physics, only relatively few cases have been reported. So far two groups of systems have been studied. The first group includes autonomous differential equations with three or more variables. These equations have been obtained either by truncating the Navier–Stokes equations[6,7] or by artificial construction.[8,9] The second group consists of nonlinear oscillators driven by external periodic force. Examples are anharmonic oscillator,[10] parametrically excited pendulum,[11] or the forced Brusselator,[12,13] which is also the subject of our paper. These two groups are related.[14,15] In particular, periodically driven systems can be written as systems of autonomous differential equations by introducing new variables.

We would like to emphasize that the second group mentioned above has the advantage that bifurcations in them may be understood as subharmonic entrainment (frequency-locking) of nonlinear oscillators and the existence of an external frequency as control parameter opens the possibility to use subharmonic stroboscopic sampling[16] to reach much higher resolution (up to 8192th subharmonic in this paper) than any present-day power spectra analysis would give.

2. THE MODEL

We study the following system of ordinary differential equations:

$$\begin{aligned} \dot{X} &= A - (B+1)X + X^2Y \\ \dot{Y} &= BX - X^2Y \end{aligned} \tag{1}$$

adding a period external force $\alpha\cos(\omega t)$ to the first equation. System (1) describes a hypothetical three-molecular chemical reaction with autocatalytic step under far from equilibrium conditions (it is usually called the Brusselator[17]). For parameter values, satisfying inequality

$$B > A^2 + 1 \tag{2}$$

it displays a limit cycle oscillation. With diffusion term added, system (1) shows a variety of spatial and temporal patterns and there exists a wide literature devoted to its study (cf. Ref. 18 and references therein).

By introducing new variables Z, U and fixing the initial conditions $Z(0) = 1$, $U(0) = 0$, the periodically forced Brusselator is equivalent to the following system of autonomous differential equations

$$\begin{aligned} \dot{X} &= A - (B+1)X + X^2Y + \alpha Z \\ \dot{Y} &= BX - X^2Y \\ \dot{Z} &= -\omega U \\ \dot{U} &= \omega Z \end{aligned} \tag{3}$$

Of course, there are many other ways to write this system, but we prefer (3), because it saves computer time owing to the absence of cosine.

In system (3) the nonlinear oscillator (1) is coupled to a linear oscillator by a linear term αZ and parameters α, ω enter the system on the same footing. Systems studied in Refs. 10 and 11 can be treated similarly. This leads us to a physical way of understanding period-doubling bifurcations in such systems. A nonlinear oscillator tends to follow the external frequency ω exactly. When the frequency difference between the limit cycle and the external force increases it adapts to $1/2$, $1/4$, $1/8$, etc. of ω (subharmonic entrainment) and finally falls into a wandering regime.

The forced Brusselator was studied first by Tomita and Kai.[12,13] They discovered a region of chaotic response on the α–ω plane, surrounded by period-doubling bifurcations. Since their work had been completed before the upsurge of papers, triggered by Feigenbaum's discovery of universality and scaling,[2] many questions remain unclear, e.g., whether the convergence rate is governed by the same Feigenbaum constant $\delta = 4.66920\ldots$, does there exist inverse sequence of chaotic bands, what is the systematics of periods 12, 40, or 44, indicated in Ref. 13 as being embedded in the chaotic region, etc. . . . Furthermore, no power spectra were given in Ref. 13, which was specially devoted to the chaotic region. In view of recent accumulation of knowledge on discrete mappings it is desirable to have a deeper understanding of systems, described by differential equations. This was our motivation to undertake a more detailed study of system (3).

3. THE METHODS

To explore the very subtle structure of chaotic bands we have to rely heavily on numerical studies. In doing so one should always be cautious not to be deceived in phenomena caused by the numerical algorithm or the computer itself. (There was a recent report[19] that two computers had given qualitatively different results for one and the same mapping.)

The main difficulty with differential equations lies in getting high enough resolution of subharmonic frequencies within reasonable computing time. This is a much more complicated task compared to the case of iterated maps, where bifurcations of rather high orders have been identified with remarkable precision. For each set of parameter values one has to integrate the system and wait for the transients to die out. The closer the bifurcation point, the longer the transient (for this critical slowing-down, see Ref. 20). Then both truncation and round-off errors may come into play.

We shall devote the methodological aspects to a separate publication elsewhere and only sketch here the methods used. Briefly speaking, we have

been working in three different domains and the results are expressed in various sections of the parameter space (A, B, α, ω) of system (3).

(a) Subharmonic stroboscopic sampling in the time domain.[16] This is a simple extension of the usual stroboscopic idea.[21] If the system undergoes period-doubling bifurcations with period $T = pT_0$, where $p = m \cdot 2^n$, $n = 0, 1, 2, \ldots$ and $T_0 = 2\pi/\omega$, then sampling at the original period T_0 would give p points on the X, Y plane. For sufficiently large p it would be very difficult to distinguish isolated points from clusters of randomly distributed points, which come from a chaotic band with a certain period, but sampling at the pth subharmonic frequency would give only one point for periodic orbit and an island of points for a chaotic band of period pT. More generally, if the system period T and sampling period T_0 are related by

$$T = \frac{p}{q} T_0 \tag{4}$$

p and q being incommensurable integers, then on the stroboscopic portrait one sees only p points (or islands) for all $q > 1$. This is a common feature of all discrete sampling methods: one can never recognize frequencies higher than the sampling frequency, but in principle can determine any subharmonics provided the total sampling time is long enough and sampled points could be resolved. If p decomposes into product of two integers i and j, then sampling at iT_0 or jT_0 essentially increases the resolution, but misuse of an integer i, which is not a factor of p, will add a spurious multiplier i in the number of periods. To be safe, one should always go from low-order subharmonics to higher ones and compare the results with power spectra analysis whenever possible.

This simple extension appears to be very powerful in reaching high resolution, the only limitation being computer time and precision. Figure 1 shows a clearly resolved period 4096 orbit, obtained by sampling at $256T_0$ and using a double precision (29 decimal digits on a Cyber computer) to avoid accumulation of round-off errors. Such high resolution surpasses any power spectra analysis available on present-day computers.

(b) Power spectra analysis in the frequency domain based on averaging 10 series of 8192 (rarely 16384) points fast Fourier transform. Although using 8192 points power spectra analysis one can hardly go beyond the 64th subharmonic without serious aliasing, power spectra are still very useful in telling chaotic bands from periodic orbits (cf. Fig. 4) and exploring fine structures of periodic orbits embedded in chaotic bands of different periodicity (cf. Fig. 8).

(c) Inspection of the trajectories in the X, Y plane or the projection of trajectories into one of the three-dimensional subspaces of X, Y, Z, U space. Having even lower resolution than the other two methods, it gives an

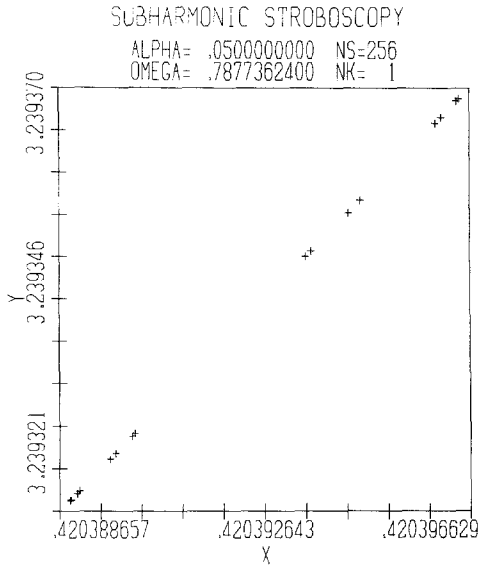

Fig. 1. Subharmonic stroboscopic portrait of a 4096P orbit ($A = 0.4$, $B = 1.2$). 256 points, sampled at $256T_0$.

intuitive feeling on the bifurcation process for low-order subharmonics, say, $p \leqslant 16$.

The results to be reported in the following sections have cost quite a large amount of computer time. To convey them as much as possible to the readers in a concise way, we need in what follows a shorthand notation. A period 32 orbit will be denoted by 32P, P standing for periodic orbit or points in the stroboscopic portrait, and a period 32 chaotic band in the inverse sequence by 32I, I standing for inverse band or islands in the portrait. What we mean by period for chaotic band will be explained in the following section, after Fig. 5.

4. HIERARCHY OF CHAOTIC BANDS

To have more comparable data we started with the same parameter values $A = 0.4$, $B = 1.2$ as in Refs. 12 and 13. Figure 2 shows the chaotic region on the α–ω plane, surrounded by period-doubling bifurcations. We shall not pay attention to the beating regime, separated by broken lines in the lower-right corner of Fig. 2. (We have discussed the nature of beating-entrainment transition elsewhere[22]). Two lines crossing the chaotic region have been examined in detail, i.e., $\alpha = 0.05$ and $\omega = 0.80$. The $\alpha = 0.05$ line was studied also in Ref. 13 and we put together our results in Table I,

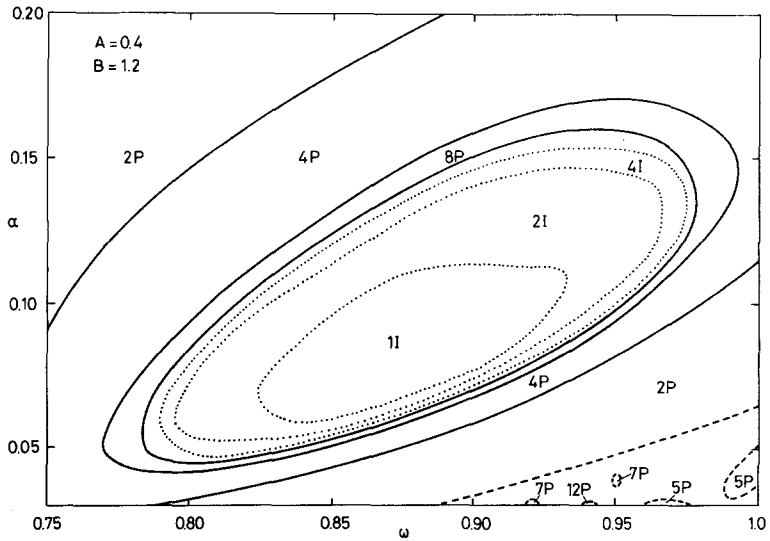

Fig. 2. Location of chaotic region in the α–ω plane: ———, boundary of periodic regime; · · · · · ·, boundary of chaotic regime; ------, boundary between periodic and beating regimes.

Table I. Hierarchy of Bifurcation Sequences along $\alpha = 0.05$ Line ($A = 0.4$, $B = 1.2$). Values of ω Are Included in Parentheses.

Primary sequence	Secondary sequences		Tertiary sequences
1P–8192P			
(0.2–.78773625)			
256I			
(.787737)			
128I	$128 \times 3 \times 1P$	(.7877408–410)	
(.7877380–428)	$128 \times 3 \times 2P$	(.7877412)	
	$128 \times 3 \times 1I$	(.7877414)	
64I	$64 \times 5 \times 1P$	(.7877496–498)	
(.787743–770)	$64 \times 5 \times 1I$	(.78775)	
	$64 \times 3 \times 1P$	(.7877575–580)	
	$64 \times 3 \times 1I$	(.7877600–605)	
32I	$32 \times 5 \times 1P$	(.787800–801)	
(.78778–.78789)	$32 \times 3 \times 1P$	(.787836–842)	
	$32 \times 3 \times 2I$	(.787843–846)	
	$32 \times 3 \times 1I$	(.787847–849)	
16I			
(.787895–.7885)			

[a] The existence of these frequencies has been indicated in Ref. 13.

Table I. *(continued)*

Primary sequence	Secondary sequences		Tertiary sequences	
8I	$8 \times 7 \times 2P$	(.7888)		
(.7886–.7909)	$8 \times 3 \times 1P^a$	(.79–.7901597)		
	$8 \times 3 \times 2P^a$	(.79015975–.790223)		
	$8 \times 3 \times 4P^a$	(.790225–250)		
	$8 \times 3 \times 4I$	(.790275)		
	$8 \times 3 \times 2I$	(.790276–278)		
	$8 \times 3 \times 1I$	(.790279–360)		
4I	$4 \times 11 \times 1P^a$	(.793–.793001)		
(.791–.8295)	$4 \times 7 \times 1P$	(.7934–.79345)		
	$4 \times 3 \times 1P^a$	(.80102–234)		
	$4 \times 3 \times 2P^a$	(.802360–2996)		
	$4 \times 3 \times 4P^a$	(.803–.803175)		
	$4 \times 3 \times 8P$	(.803177–195)		
	$4 \times 3 \times 16P^a$	(.803197–200)		
	$4 \times 3 \times 4I$	(.80322–323)	$48 \times 3 \times 2P$	(.80321)
	$4 \times 3 \times 2I$	(.80324–336)	$24 \times 3 \times 1I$	(.80331)
	$4 \times 3 \times 1I$	(.80338–440)	$24 \times 3 \times 2I$	(.80332)
	$4 \times 3 \times 1I$	(.818–.8192)	$12 \times 5 \times 2I$	(.81925)
	$4 \times 3 \times 2I$	(.81928–934)		
	$4 \times 3 \times 4I$	(.81936–938)		
	$4 \times 3 \times 8P^a$	(.8194–.81943)		
	$4 \times 3 \times 4P^a$	(.819433–728)		
	$4 \times 3 \times 2P^a$	(.819731–.8202)		
	$4 \times 3 \times 1P^a$	(.82025–.8214)		
	$4 \times 3 \times 1P$	(.8245–.82599)		
8I	$8 \times 3 \times 1I$	(.831–.83102)		
(.83–.8325)	$8 \times 3 \times 2I$	(.83104)		
	$8 \times 3 \times 4P$	(.83106)		
	$8 \times 3 \times 2P$	(.8311–.83112)		
	$8 \times 3 \times 1P$	(.83114–.83120)		
	$8 \times 5 \times 1I$	(.83194–.83196)		
	$8 \times 5 \times 4P$	(.83198)		
	?			
	$8 \times 5 \times 1P^a$	(.832–.832005)		
16I				
(.8327–.83304)				
32I				
(.83306–.83314)				
64I				
(.83315–.83317)				
128I				
(.833175)				
256I				
(.83318)				
128P–2P				
(.83319–.950475)				

Table II. A Period-Doubling Bifurcation Sequence in Eqs. (3)

n	Period	Range in ω		ω_n	δ_n
1	1		− 0.39820	0.398205	5.53
2	2	0.39821	− 0.71305	0.7130625	4.24
3	4	0.713075	− 0.769996	0.7699998	4.02
4	8	0.770000	− 0.78337	0.783435	4.46
5	16	0.78350	− 0.786752	0.786776	4.41
6	32	0.78680	− 0.78752	0.787525	5.40
7	64	0.78753	− 0.78769	0.787695	4.04
8	128	0.78770	− 0.787726	0.7877265	4.88
9	256	0.787727	− 0.787734	0.78773425	4.92
10	512	0.7877345	− 0.7877358	0.78773585	
11	1024	0.7877359	− 0.78773615	0.787736175	
12	2048	0.78773620			
13	4096	0.78773624			
14	8192	0.78773625			

where frequencies, whose existence was indicated in Ref. 13, were marked by a superscript a. With our high resolution we succeeded in recognizing systematically many inverse bands within the chaotic region and in seeing a lot of secondary bifurcation sequences with both direct and inverse segments.

As regards the primary direct sequence we have located rather high-order bifurcations up to $p = 8192$ (see Table II). To our knowledge, this is the longest period-doubling sequence ever identified for a system of nonlinear differential equations. The estimate of the convergence rate

$$\delta_n = \frac{\omega_n - \omega_{n+1}}{\omega_{n+1} - \omega_{n+2}} \tag{5}$$

given in the last column of Table II, shows that most probably we have here the same Feigenbaum constant δ. Critical slowing-down near every bifurcation point has prevented us from locating the boundaries of each period with high precision and we simply take the middle point between two last seen consecutive periods to be the boundary. Thus we cannot expect a better estimate of δ in this way.

In the third column of Table I there are a few indications on the existence of perodicities of the third level, embedded in chaotic bands of the secondary inverse sequence. This is indeed the case, as it can be seen more clearly from the results along the $\omega = 0.80$ line, summarized in Table III.

This hierarchy structure is visualized in Fig. 3. It shows schematically the bifurcations at fixed external frequency $\omega = 0.80$. When the amplitude

Table III. Hierarchy of Bifurcation Sequences along $\omega = 0.8$ line ($A = 0.4$, $B = 1.2$). Values of α Are Included in Parentheses.

Primary sequence	Secondary sequences		Tertiary sequences	
2P–128P				
(.01–.04696)				
32I	$32 \times 3 \times 1$P	(.04700)		
(.04698–.04701)				
16I	$16 \times 3 \times 1$P	(.0471000–055)		
(.047025–.047197)	$16 \times 3 \times 2$P	(.0471100–114)		
	$16 \times 3 \times 4$P	(.0471116–128)		
	$16 \times 3 \times 2$I	(.047113)	$96 \times 3 \times 1$I	(.0471135)
	$16 \times 3 \times 1$I	(.047114–118)		
8I	$8 \times 3 \times 1$P	(.047591–637)		
(.047198–.0484)	$8 \times 3 \times 2$P	(.0476380–575)		
	$8 \times 3 \times 4$P	(.0476580–625)		
	$8 \times 3 \times 8$P	(.0476630–640)		
	$8 \times 3 \times 16$P	(.0476641–642)		
	$8 \times 3 \times 32$P	(.0476643)		
	$8 \times 3 \times 8$I	(.0476644–649)		
	$8 \times 3 \times 4$I	(.0476651–654)	$96 \times 3 \times 1$P	(.0476650)
	$8 \times 3 \times 2$I	(.0476656–699)	$48 \times 5 \times 1$P	(.0476662)
			$48 \times 3 \times 1$P	(.0476673–75)
			$48 \times 3 \times 2$P	(.0476676)
			$48 \times 3 \times 1$I	(.0476677–80)
	$8 \times 3 \times 1$I	(.047670–688)	$24 \times 3 \times 1$I	(.047679–680)
4I	$4 \times 7 \times 1$P	(.048495)		
(.04845–.0535)	$4 \times 5 \times 1$P	(.048945–959)		
	$4 \times 5 \times 2$P	(.04896–.04900525)		
	$4 \times 5 \times 4$P	(.049010–011)		
	$4 \times 5 \times 8$P	(.049012)		
	$4 \times 5 \times 2$I	(.049015)		
	$4 \times 5 \times 1$I	(.049016–025)	$20 \times 5 \times 1$P	(.0490218–20)
2I	$2 \times 7 \times 1$P	(.05580–585)		
(.0545–.0725)	$2 \times 7 \times 2$P	(.055860–875)		
	$2 \times 7 \times 4$P	(.05588)		
	$2 \times 7 \times 8$P	(.055885)		
	$2 \times 7 \times 2$I	(.05589)		
	$2 \times 7 \times 1$I	(.055895–920)		
	$2 \times 7 \times 8$P	(.0704)		
	?			
	$2 \times 7 \times 1$P	(.0705)		
4I	$4 \times 3 \times 1$I	(.0770–772)		
(.0735–.0809)	$4 \times 3 \times 2$P	(.0773)		
	$4 \times 3 \times 1$P	(.0775–776)		
	$4 \times 5 \times 1$P	(.0795)		
8I	$8 \times 5 \times 1$P	(.08145)		
(.08092–.0825)	$8 \times 3 \times 1$I	(.0817)		
	$8 \times 3 \times 2$P	(.08175)		
	$8 \times 3 \times 1$P	(.08180–185)		

Table III. *(continued)*

Primary sequence	Secondary sequences		Tertiary sequences
16I	$16 \times 3 \times 1$I	(.082671–682)	$48 \times 7 \times 1$P (.08268)
(.08255–.08285)	$16 \times 3 \times 8$P	(.082683)	
	$16 \times 3 \times 4$P	(.082684–685)	
	$16 \times 3 \times 2$P	(.0826900–925)	
	$16 \times 3 \times 1$P	(.082695–706)	
32I	$32 \times 5 \times 1$P	(.082902)	
(.08286–.082914)	$32 \times 7 \times 1$P	(.08291)	
64I			
(.082916–.08293)			
128I	$128 \times 3 \times 1$P	(.0829310–312)	
(.0829302–327)	$128 \times 7 \times 1$P	(.0829318)	
256I	$256 \times 3 \times 1$P	(.082933)	
(.0829332–338)			
512P–1P			
(.082934–20.0)			

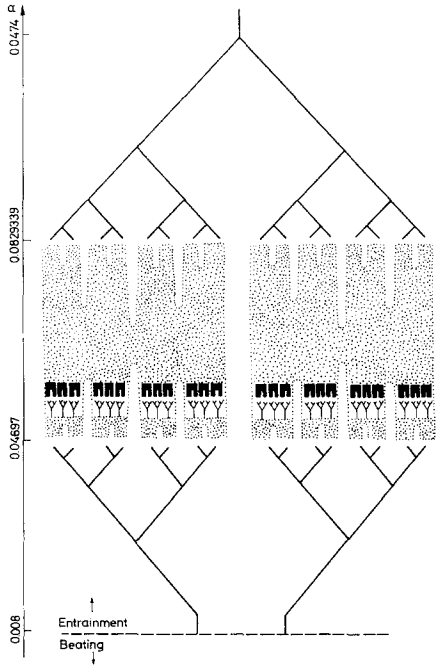

Fig. 3. Hierarchy of period-doubling bifurcation sequences (schematic, not to scale). Only one secondary sequence embedded in a 8I band is shown.

α is very small the periodic force cannot entrain the system and there exist two independent frequencies (beating regime, not shown in Fig. 3). With α increasing the system passes through a sharp beating-entrainment transition (horizontal broken line in Fig. 3) and a period-doubling sequence takes place with $p = 2$. Its inverse sequence merges with that of another period-doubling sequence, which ends with only one period when the external force takes over. Therefore the chaotic behavior appears as a compromise between two trends: at small α the limit cycle tries to show itself up, at large α the external force dominates, and chaotic behavior exists in between as a new regime of nonlinear oscillation. This is the physical understanding of period-doubling bifurcation and associated chaotic behavior, which we mentioned at the end of the Introduction.

Periodic and chaotic orbits can be distinguished best by subharmonic stroboscopic sampling.[16] For not-very-high-order subharmonics the distinctions are clearly expressed in the power spectra and trajectories in the X, Y plane. In Figs. 4 and 5 we compare the spectra and trajectories of 2P, 4P, 8P, 16P, and 32P orbits with that of 2I, 4I, 8I, 16I, and 32I orbits. What is remarkable are the sharp peaks in the broad-band spectra of chaotic orbits. This has been seen before[9] and called phase coherence in Ref. 15. It seems to be related to the splitting of strange attractor, seen in Fig. 5f–j. In all these figures a trajectory was plotted for 305 periods. If we drew many more periods, only a winded black strip would remain in Fig. 5f–j. It is this number of windings which determines the period of a chaotic band. (Notice: in both Fig. 5e and 5j the splitting of the outermost loop into two has not been well resolved.)

The $\alpha = 0.05$ and $\omega = 0.8$ lines were chosen before we located the position of 1I, 2I, 4I, . . . regions in the α–ω plane, marked by dotted lines in Fig. 2. Thus the $\alpha = 0.05$ line crosses only 4I and higher bands, the $\omega = 0.8$ line crosses only 2I and higher bands, both missing the 1I region. By increasing α to 0.08 we drew the trajectories of 1I, 2I, and 4I chaotic orbits, as shown in Fig. 6, which give a better feeling of how a "strange attractor"[4] splits.

Now we turn to the systematics of periodicities, embedded in chaotic bands. In a kI chaotic band periodicities of the next level always appear to have k as a factor. Therefore, simple period 3, 5, or 7 may be found only in 1I band. In a 8I band one never sees period 12, 20, or 28, because the smallest period with factor 3, 5, or 7 would be 24, 40, or 56, respectively. In general, one may have period

$$P = k \cdot m \cdot 2^n \tag{6}$$

[4] We use this term to name the apparently chaotic object seen numerically.

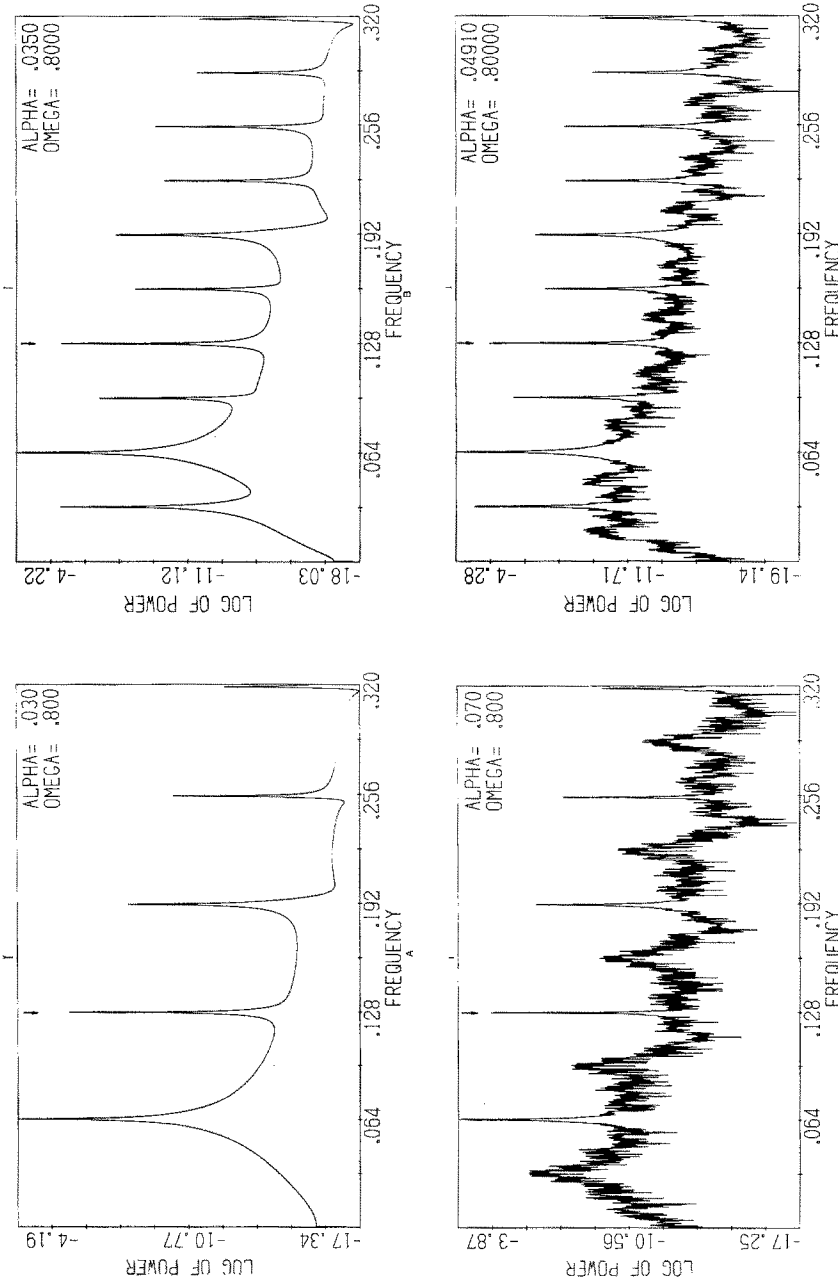

Fig. 4. Power spectra of periodic and chaotic orbits. (a) 2P, (b) 4P, (c) 8P, (d) 16P, (e) 32P, (f) 2I, (g) 4I, (h) 8I, (i) 16I, (j) 32I.

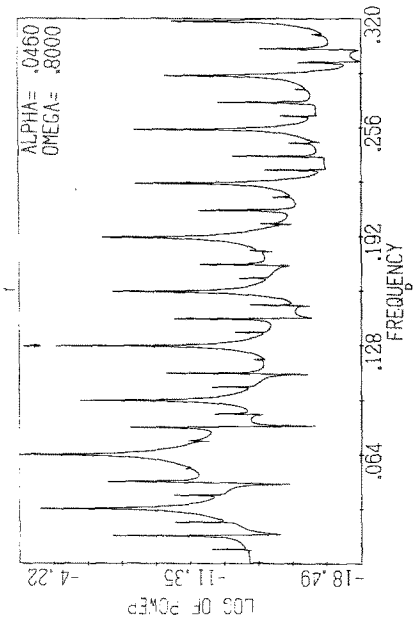
ALPHA= .0460
OMEGA= .8000
LOG OF POWER
-18.49
-11.35
-4.22
.064
.128
.192
.256
.320
FREQUENCY
D

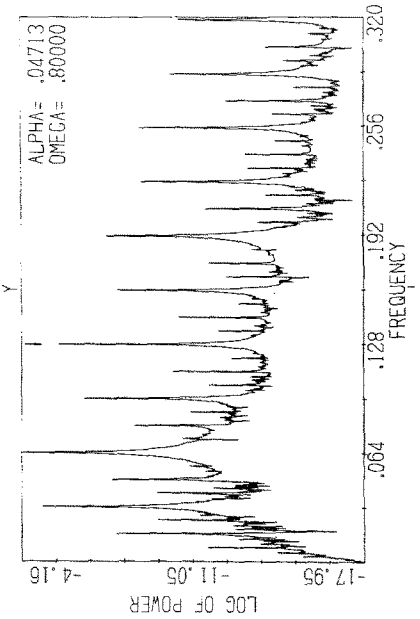
ALPHA= .04713
OMEGA= .80000
LOG OF POWER
-17.95
-11.05
-4.16
.064
.128
.192
.256
.320
FREQUENCY
B

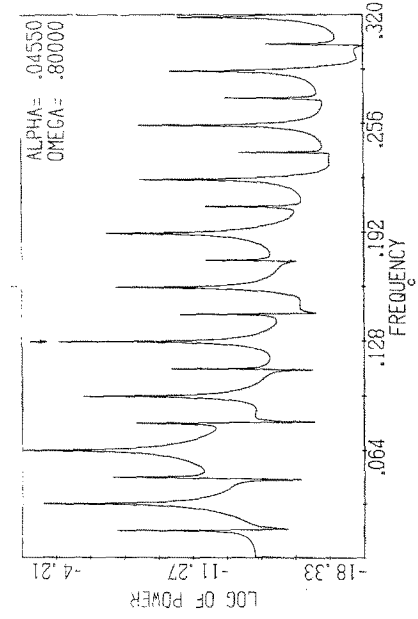
ALPHA= .04550
OMEGA= .80000
LOG OF POWER
-18.33
-11.27
-4.21
.064
.128
.192
.256
.320
FREQUENCY
C

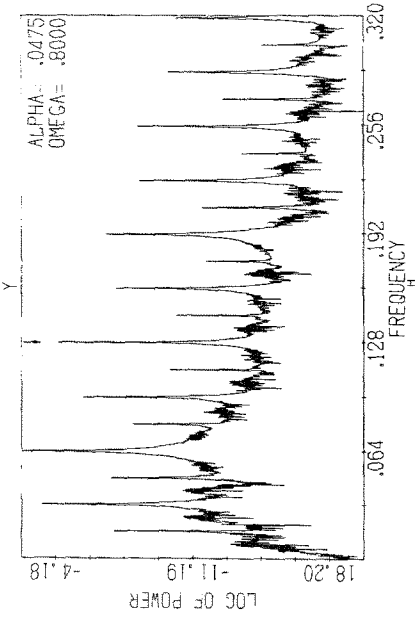
ALPHA= .0475
OMEGA= .8000
LOG OF POWER
18.20
-11.19
-4.18
.064
.128
.192
.256
.320
FREQUENCY
A

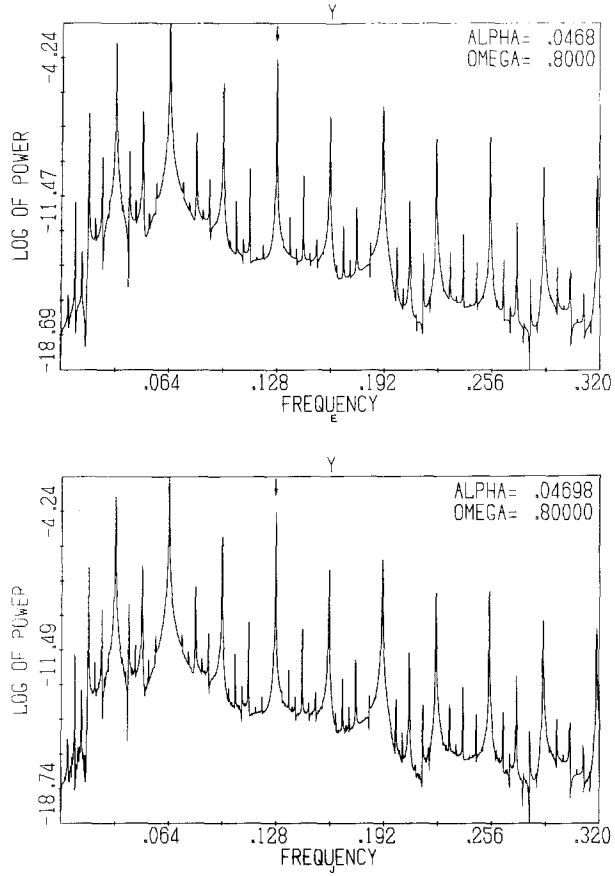

where k is the period of the underlying chaotic band, $m = 3, 5, 7, 11, \ldots$, and $n = 0, 1, 2, \ldots$. This refers to the periodic orbits in the direct sequence as well as to the period of chaotic bands in the inverse sequence. In all cases studied so far, we have not encountered any exception to this rule.

Figure 7 shows schematically the structure of a 8I band which is the one emphasized in Fig. 3 and has been searched in more detail. A direct bifurcation sequence with period $8.3.2^n$, $n = 0$–5, and the associated inverse sequence with period $8.3.2^n$, $n = 0$–3, were located explicitly. Within the 24I and 48I chaotic bands of this secondary sequence, shorter tertiary sequences with 24 or 48 as factor in their period were identified.

This hierarchy structure may be interpreted by splitting and shrinking of the strange attractor at certain parameter values. After primary splitting one can imagine an arm of the strange attractor as a rope made of infinite number of threads. At certain parameter values threads in each arm shrink

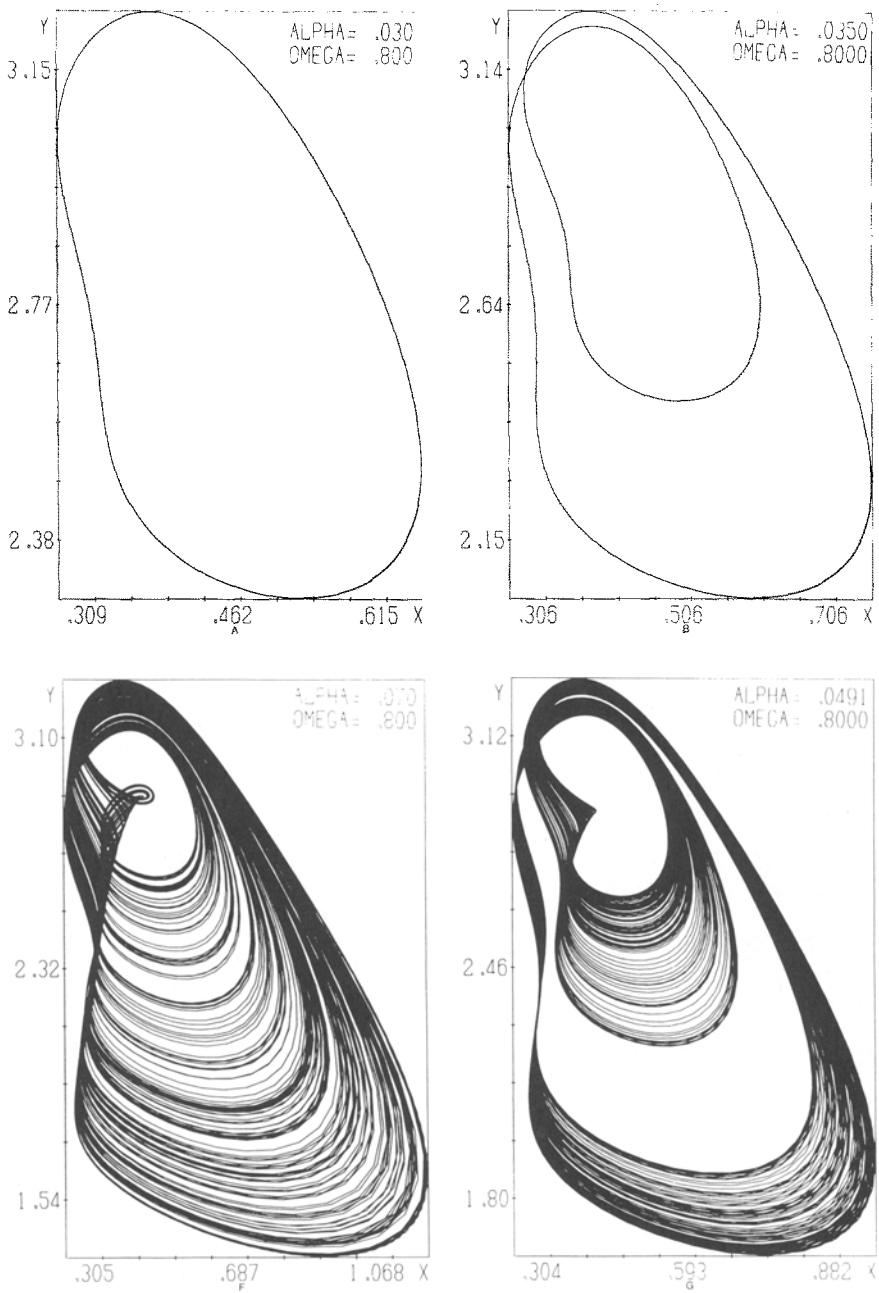

Fig. 5. Trajectories in the X, Y plane. (a) 2P, (b) 4P, (c) 8P, (d) 16P, (e) 32P, (f) 2I, (g) 4I, (h) 8I, (i) 16I, (j) 32I.

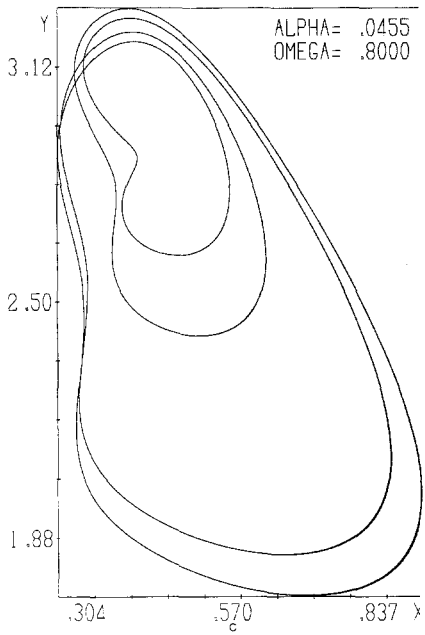
Y
3.12
2.50
1.88
ALPHA= .0455
OMEGA= .8000
.304
.570
.837
X
C

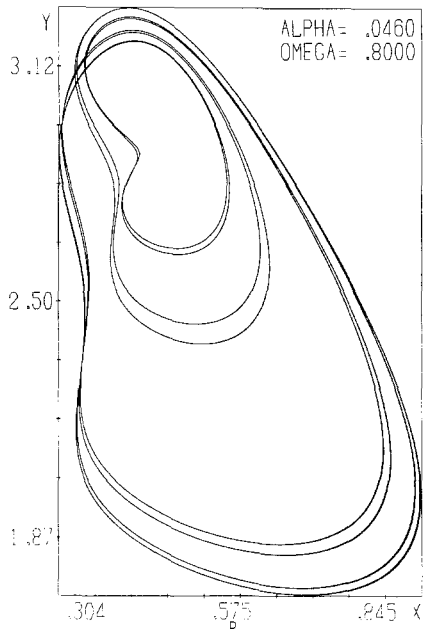
Y
3.12
2.50
ALPHA= .0460
OMEGA= .8000
.304
.575
.845
X
D

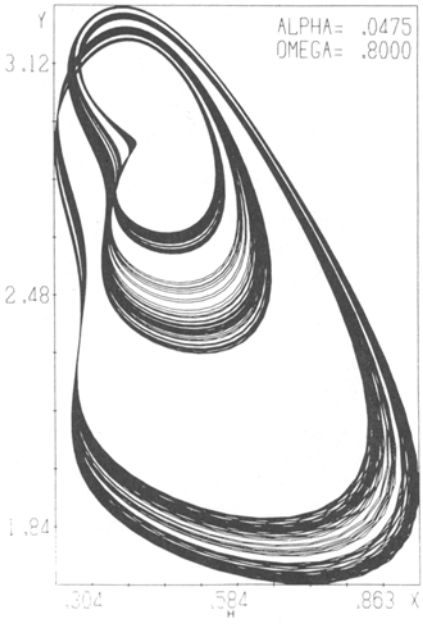
Y
3.12
2.48
1.84
ALPHA= .0475
OMEGA= .8000
.304
.584
.863
X
H

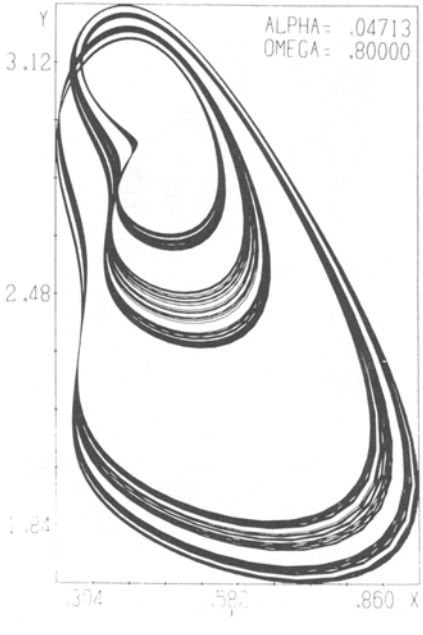
Y
3.12
2.48
ALPHA= .04713
OMEGA= .80000
.304
.860
X

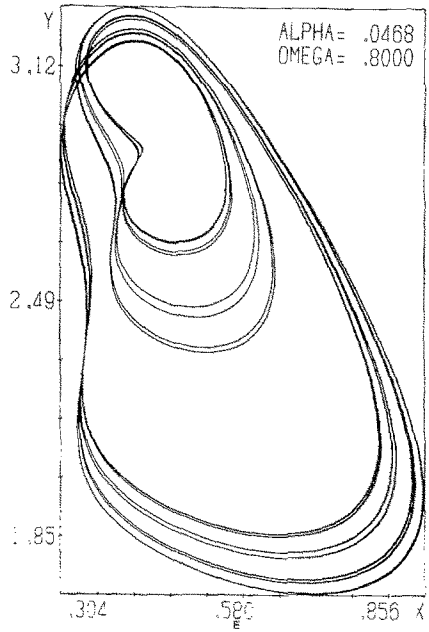
Y
3.12
2.49
1.85
ALPHA= .0468
OMEGA= .8000
.856 X

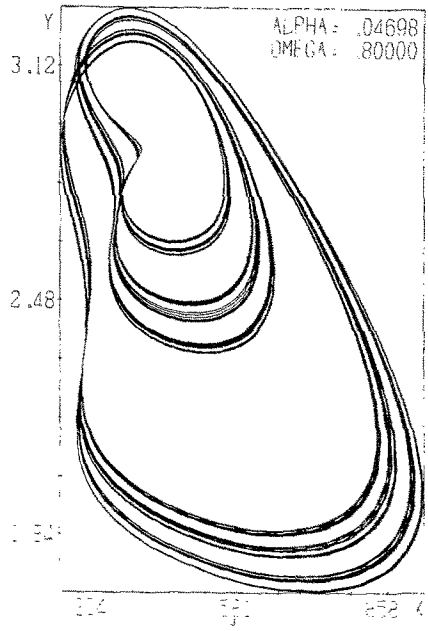
Y
3.12
2.48
ALPHA= .04698
OMEGA= .80000

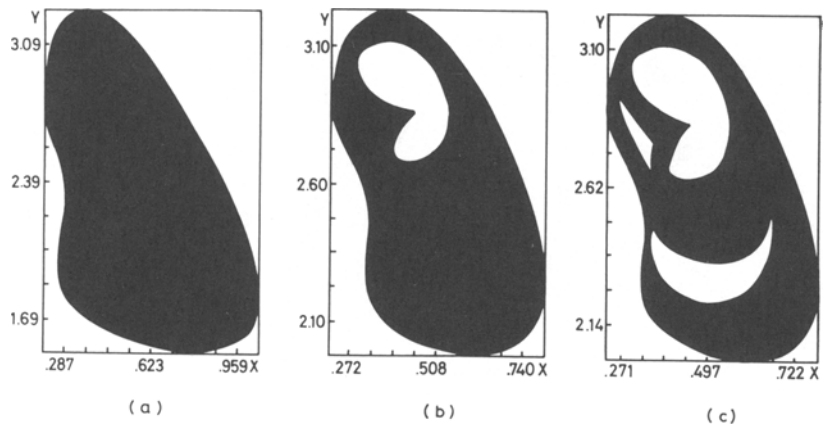

Fig. 6. Strange attractors ($A = 0.4$, $B = 1.2$). (a) 1I ($\alpha = 0.08$, $\omega = 0.86$); (b) 2I ($\alpha = 0.08$, $\omega = 0.91$); (c) 4I ($\alpha = 0.08$, $\omega = 0.915$).

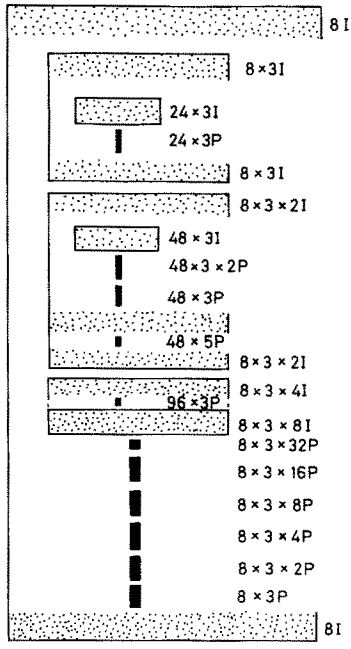

Fig. 7. Secondary and tertiary bifurcation sequences, embedded in a 8I band (schematic).

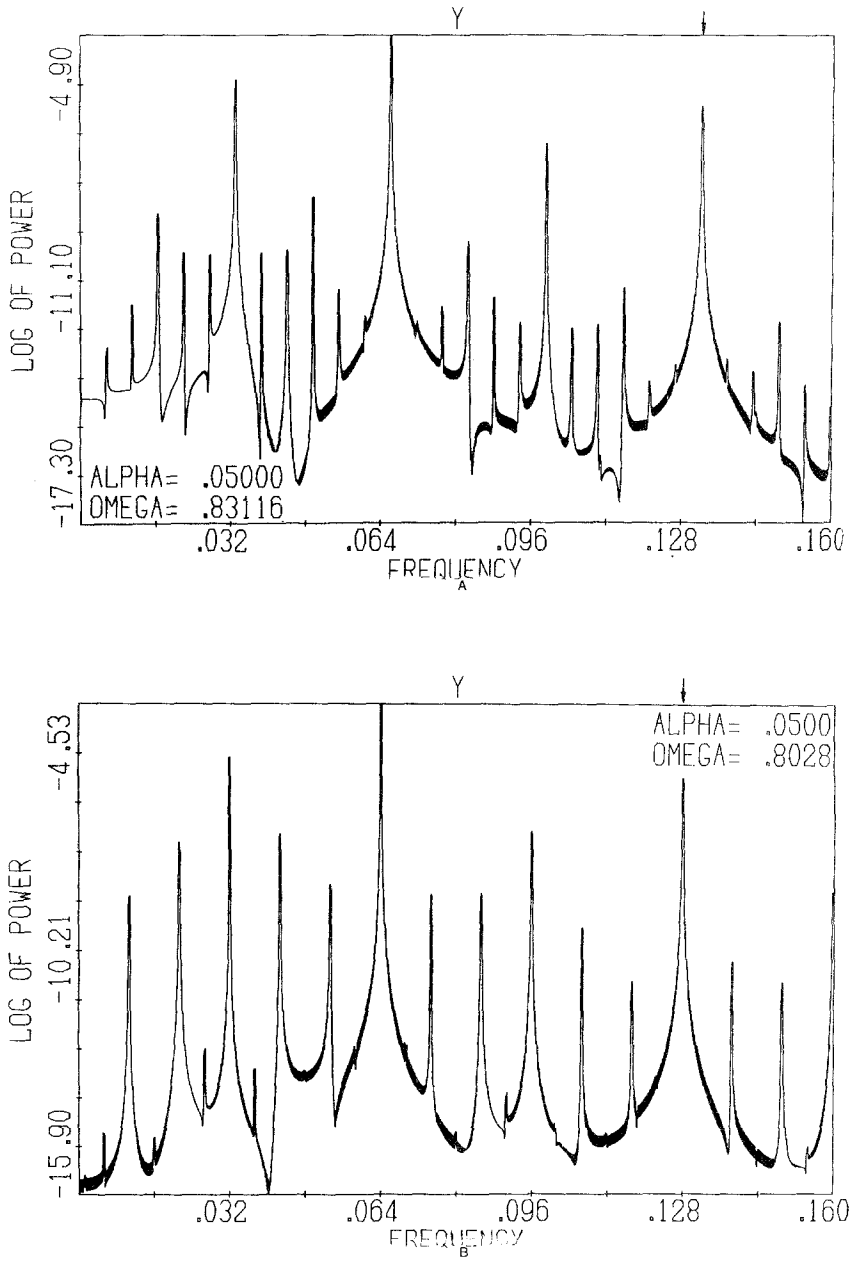

Fig. 8. Power spectra of 24P orbits embedded in different chaotic bands. An arrow indicates the fundamental frequency. (a) $8 \times 3P$ in 8I band; (b) $4 \times 3 \times 2P$ in 4I band.

simultaneously into a finite number of threads, producing thereby a periodic orbit. This process repeats at each level on smaller and smaller scales. It reflects in the power spectra as well. For example, 24P orbits embedded in 8I or 4I chaotic bands can easily be identified for having a 8×3 or $4 \times 3 \times 2$ fine structure (see Fig. 8).

To conclude this section, we make two remarks. First, one can estimate the convergence rate of primary chaotic bands and secondary direct sequences, using data given in Tables I and III. Everywhere we find almost the same range of δ value. Second, being impossible to make an overall search by very small steps, we certainly have missed many periodicities. $m = 3, 5, 7$ in formula (6) correspond to most easily found periods. This explains why there are so many of them in Tables I and III. There is only one case with $m = 11$ and we have nothing to say about $m = 9$.

5. FINITENESS OF CHAOTIC REGION IN PARAMETER SPACE

It is interesting to ask what happens with the chaotic region if we make the original system (1) nearer to or further away from the time-independent

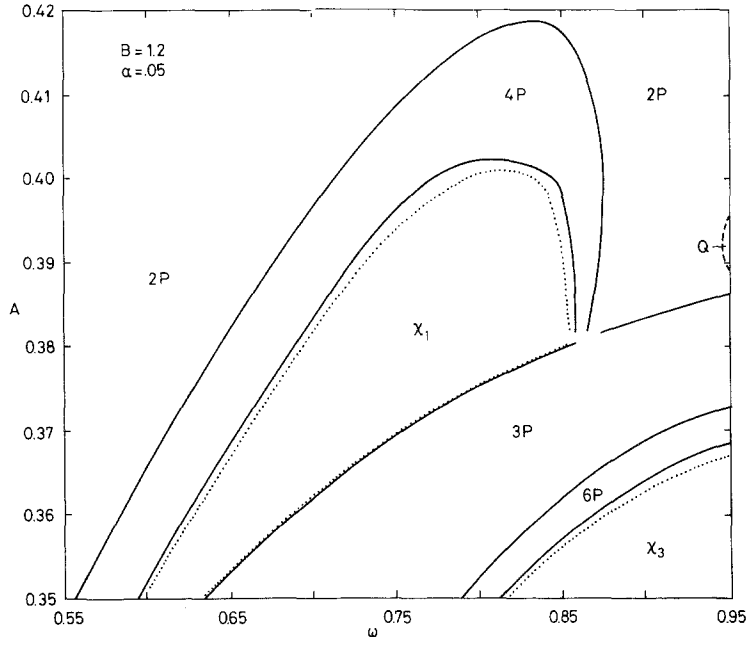

Fig. 9. Location of chaotic regions in the A–ω plane: ———, boundary of periodic regime; · · · · · · , boundary of chaotic regime; ------, boundary between periodic and beating (Q) regime.

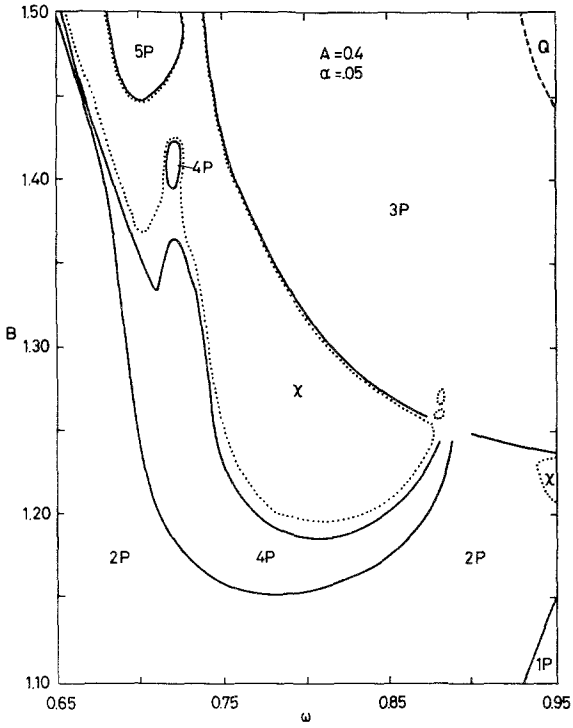

Fig. 10. Location of chaotic regions in the B–ω plane: ———, boundary of periodic regime; · · · · · ·, boundary of chaotic regime; ------, boundary between periodic and beating (Q) regime.

stationary state, i.e., if we weaken or strengthen the inequality (2). The A–ω plane for fixed B, α (Fig. 9) and the B–ω plane with A, α fixed (Fig. 10) look more complicated than the α–ω plane (Fig. 2).

In the lower-right corner of Fig. 9 we see a part of another chaotic region, surrounded by 3.2^n ($n = 0, 1, 2, \ldots$) type period-doubling bifurcations. We have looked at it closer along the $A = 0.36$ and $\omega = 0.9$ lines. It seems to have a structure similar to what we described in the previous section, if one changes all periods by a factor of 3.

The 3P regime occupies an even more conspicuous place in the B–ω plane (Fig. 10). In both Figs. 9 and 10 the 3P goes into chaotic region directly, without any period-doubling sequence in between (probably there is a 3I intermediate state, which can hardly be distinguished from very long transients of 3P). It is unclear to us whether this fact is relevant to the cubic nonlinearity in the particular model or it is a common feature shared by other systems too. It might be a manifestation of some analog to the

Li–Yorke theorem,[23] which was proved onlv for one-dimensional mappings and says that period 3 (then generalized to 5, 7, etc.) always implies chaos. Anyhow, the role of period 3 in the case of differential equations requires further scrutiny. The same comment holds for 5P in Fig. 10.

The structure of a small region near the intersection of 3P, 2^nP, and chaotic regimes on both Figs. 9 and 10 remain unresolved. We leave this question for future study.

A comparison of Figs. 2, 9, and 10 suggests to us a conjecture that the chaotic regime occupies finite region in the parameter space. This seems not to be in disagreement with recent observations on the Lorenz model.[24] If, in addition, chaotic bands and periodicities embedded in them are nested one into another, then so-called "window structure" of periodic orbits, mentioned by many authors, e.g., Ref. 13, would be a simple consequence of this nesting. Our data in Tables I and III support this nested character of secondary bifurcation sequences, e.g., the order of all direct and inverse sequences are reversed at two opposite sides of the parameter range. The same seems to be true for tertiary sequences, but one needs finer data to be confident.

6. DISCUSSION

The forced Brusselator shows very complicated bifurcation and chaotic behavior in certain regions of the control parameter space. Still if only one parameter varies, we see many features common to one-dimensional discrete mappings. Phenomena related to the role of 3P orbits require further study. The hierarchy structure of bifurcation sequences should be observable also in mappings and other nonlinear differential equations. In other words, we expect not only the existence of a few universal numerical characteristics, but also the universality of the essential overall structure of the bifurcation scheme.

Having in mind the results reported in this paper, we can review other systems in retrospect.

In the 5-mode truncated Navier–Stokes equations,[7] most probably what was observed was a primary direct sequence up to 32P and a secondary sequence with $m = 3$, embedded in 1I or 2I chaotic band. A power spectrum analysis would help to reveal its identity.

In the Rössler model the presence of 1P to 8P and 1I to 8I bands has been observed clearly.[9] The authors of Ref. 9 have seen also 16P and 16I bands. Owing to limited precision of the analog computer, no boundaries and δ values were estimated.

In the parametrically excited pendulum,[11] a direct sequence from 1P to 32P was reported and two points belong to 2I and 4I bands observed. It

was noticed in Ref. 11 that at the far end of the parameter axis 1P orbit there appears again what would be another indication on finiteness of chaotic region.

In all cases cited only one parameter has been varied. It would be very useful to enlarge the parameter space, as our results have shown, but what is the best (or minimal) parameter space for a given dynamical system to explore the bifurcation and chaotic behavior in all its complexity and variety?

To conclude this paper we would like to emphasize once more our understanding of period-doubling bifurcations and the associated chaos as a new chapter in the theory of nonlinear oscillation, although it certainly throws new lights on fundamental problems of statistical physics.

ACKNOWLEDGMENT

The main body of this research has been done during our stay at the Instituts Internationaux de Physique et de Chimie, fondés par E. Solvay, in Brussels, and the final manuscript written while visiting the Service de Physique Théorique, CEA–Saclay. The first author (H.) thanks these institutions for hospitality and support. He thanks Drs. I. Prigogine, G. Nicolis, L. Reichl, D. K. Kondepudi, and M. Feigenbaum for discussions and comments at different occasions. Dr. J. B. McLaughlin and V. Franceschini sent their reprints to H. Dr. E. Brézin kindly read the manuscript. We express our gratitude to all of them.

REFERENCES

1. P. Collet and J.-P. Eckmann, *Iterated Maps on the Interval as Dynamical Systems* (Birkhäuser, Basel, 1980).
2. M. J. Feigenbaum, *J. Stat. Phys.* **19**:25 (1978); **21**:669 (1979).
3. B. A. Huberman and J. Rudnick, *Phys. Rev. Lett.* **45**:154 (1980).
4. M. J. Feigenbaum, *Commun. Math. Phys.* **77**:65 (1980); B. A. Huberman and A. B. Zisook, *Phys. Rev. Lett.* **46**:626 (1981); P. Collet, J.-P. Eckmann, and L. Thomas, *Commun. Math. Phys.* **81**:261 (1981); M. Nauenberg and J. Rudnick, Universality and the power spectrum at the onset of chaos, UCSC preprint 81/137.
5. P. Collet, J.-P. Eckmann, and H. Koch, *Commun. Math. Phys.* **25**:1 (1981).
6. E. N. Lorenz, *J. Atmos. Sci.* **20**:130 (1963); V. Franceschini, *J. Stat. Phys.* **22**:397 (1980).
7. V. Franceschini and C. Tebaldi, *J. Stat. Phys.* **21**:707 (1979).
8. O. E. Rössler, *Ann. N.Y. Acad. Sci.* **316**:376 (1979).
9. J. Crutchfield, D. Farmer, N. Parcard, R. Shaw, G. Jones, and R. J. Donnelly, *Phys. Lett.* **76A**:1 (1980).
10. B. A. Hubermann and J. P. Crutchfield, *Phys. Rev. Lett.* **43**:1743 (1979).
11. J. B. McLaughlin, *J. Stat. Phys.* **24**:377 (1981).
12. T. Kai and K. Tomita, *Progr. Theor. Phys.* **61**:54 (1979).
13. K. Tomita and T. Kai, *J. Stat. Phys.* **21**:65 (1979).

14. P. Coullet, C. Tresser, and A. Arnéodo, *Phys. Lett.* **72A**:268 (1979).
15. D. Farmer, J. Crutchfield, H. Froehling, N. Parcard, and R. Shaw, *Ann. N.Y. Acad. Sci.* **357**:453 (1980).
16. B.-L. Hao and S.-Y. Zhang, *Phys. Lett.* **87A**:267 (1982).
17. J. J. Tyson, *J. Chem. Phys.* **58**:3919 (1973).
18. G. Nicolis and I. Prigogine, *Self-Organization in Non-Equilibrium Systems* (Wiley, New York, 1977).
19. J. H. Curry, *Commun. Math. Phys.* **68**:129 (1979).
20. B.-L. Hao, *Phys. Lett.* **86A**:267 (1981).
21. N. Minorsky, *Théorie des Oscillations* (Gauthier-Villars, Paris, 1967); K. Tomita and T. Kai, *Phys. Lett.* **66A**:91 (1978).
22. B.-L. Hao, Two kinds of entrainment-beating transitions in a driven limit-cycle oscillator, *J. Theor. Biol.* (to appear).
23. T. Y. Li and J. A. Yorke, *Am. Math. Monthly* **82**:985 (1975).
24. I. Simada and T. Nagashima, *Progr. Theor. Phys.* **59**:1033 (1978); K. A. Robbins, *SIAM J. Appl. Math.* **36**:457 (1979).